Molecular BioSystems

Accepted Manuscript

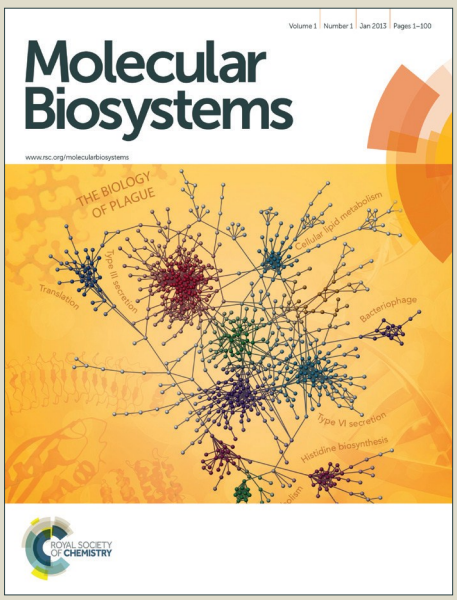

ROYAL SOCIETY OF CHEMISTRY

www.rsc.org/molecularbiosystems

TOC Graphic:

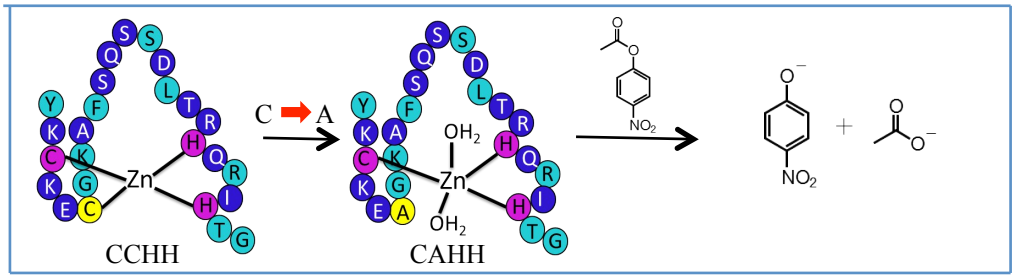

Revisiting and re-engineering the Classical Zinc Finger Peptide:

Consensus Peptide-1 (CP-1)

Angelique N. Besold,[a] Leland R. Widger,[b] Frances Namuswe,[b] Jamie L. Michalek,[a]

Sarah L. J. Michel,[a,*] and David P. Goldberg[b,*]

[a] Department of Pharmaceutical Sciences, School of Pharmacy, University of Maryland, Baltimore, MD 21201, USA

[b]Department of Chemistry, Johns Hopkins University, Baltimore, MD 21218, USA

*Corresponding authors: SLJM: smichel@rx.umaryland.edu, 410-706-7038; DPG: dpg@jhu.edu, 410-516-6658

Abstract

Zinc plays key structural and catalytic roles in biology. Structural zinc sites are often referred to as zinc finger (ZF) sites, and the classical ZF contains a Cys_2His_2 motif that is involved in coordinating Zn(II). An optimized Cys_2His_2 ZF, named consensus peptide 1 (CP-1), was identified more than 20 years ago using a limited set of sequenced proteins. We have reexamined the CP-1 sequence, using our current, much larger database of sequenced proteins that have been identified from high-throughput sequencing methods, and found the sequence to be largely unchanged. The CCHH ligand set of CP-1 was then altered to a CAHH motif to impart hydrolytic activity. This ligand set mimics the His_2Cys ligand set of peptide deformylase (PDF), a hydrolytically active M(II)-centered (M = Zn or Fe) protein. The resultant peptide [CP-1(CAHH)] was evaluated for its ability to coordinate Zn(II) and Co(II) ions, adopt secondary structure, and promote hydrolysis. CP-1(CAHH) was found to coordinate Co(II) and Zn(II) and a pentacoordinate geometry for Co(II)-CP-1(CAHH) was implicated from UV-vis data. This suggests a $His_2Cys(H_2O)_2$ environment at the metal center. The Zn(II)-bound CP-1(CAHH) was shown to adopt partial secondary structure by 1-D ^1H NMR spectroscopy. Both Zn(II)-CP-1(CAHH) and Co(II)-CP-1(CAHH) show good hydrolytic activity toward the test substrate 4-nitrophenyl acetate, exhibiting faster rates than most active synthetic Zn(II) complexes.

Introduction

It is estimated that one-third of all proteins are bound to metal ions.[1-4] One key metal ion for proteins is zinc, which can play either a structural or a catalytic role.[5-10] The group of proteins for which zinc plays a structural role are collectively called zinc finger (ZF) proteins.[11, 12] These proteins are highly abundant (e.g. 3-10% of the human genome encodes for ZF proteins) and are identified in genomes based upon the presence of cysteine and histidine rich domains.[11, 12] ZF proteins utilize these cysteine and/or histidine ligands to coordinate zinc(II) into a tetrahedral geometry and fold into a three-dimensional structure. Once folded, the ZF can function – i.e. bind to DNA, RNA or another protein.[11, 13-21] The best-studied class of ZFs are the 'classical' ZFs. These ZFs bind zinc(II) using a Cys_2His_2 (CCHH) motif and adopt a ββα fold upon zinc coordination (Fig. 1). [6, 11-13, 22, 23] Since the discovery of classical ZFs in the late 1980s, at least fourteen additional classes of (non-classical) ZFs have been identified. [11, 12] Each class is delineated by the ligands that coordinate zinc and the structure that the peptide adopts upon zinc(II) coordination.[11,13-21]

In all ZF proteins, the zinc binding domains are well defined and make up smaller domains of the larger protein.[11, 12, 22, 24-26] As a result, these ZF domains can be isolated independently of the rest of the protein, and still bind zinc ions and fold.[11, 12, 26] This modular nature of ZF domains has led to many successful efforts to mimic ZFs by preparing short peptides that match the sequence of a specific zinc(II) binding domain of a particular protein.[27-30] [19, 31] In addition, shortly after the identification of the classical ZF by Berg and co-workers in 1987,[32] an optimal or consensus sequence was defined for this class of ZF proteins by aligning the sequences of the few known classical ZFs and identifying a sequence based upon the most prevalent amino acid within each position of the sequence alignment. This sequence, named

consensus peptide-1 (or CP-1), [33] was determined by manually aligning all of the sequences of classical zinc finger proteins and identifying which residue occurs most frequently at each position. CP-1 was subsequently prepared and characterized and shown to exhibit maximal zinc(II) binding affinity and optimal protein folding.[33-36]

CP-1 was defined in 1991, before any major eukaryotic genomes (e.g. *homo sapiens)* had been published and before modern methods of sequence analysis had become readily available, yet continues to be the sequence utilized as the model classical ZF peptide. Here, we sought to determine whether this consensus sequence remained the same in 2015, given the proliferation of sequenced genomes since 1991. Remarkably, we found that there are minimal changes to the CP-1 sequence, despite the explosion of available protein sequence data.

We then sought to determine if CP-1 could be modified to promote hydrolysis. There has long been an interest in utilizing ZF peptides in protein design, because their small size, ease of synthesis, modular nature and metal-binding properties them attractive building blocks.[25, 37] The conversion of a structural ZF site to a catalytic Zn site is one area of protein design of particular interest for ZFs, because zinc can have a catalytic role in biology. Proteins that utilize zinc sites for a catalytic role typically coordinate zinc(II) using three amino acid ligands, usually histidine, aspartate, glutamate and/or cysteine. Importantly, these catalytic zinc centers usually contain one or more open coordination sites that are absent in structural ZFs, and which allow for binding of substrates and small molecule (e.g. H_2O) co-factors to promote reactivity.[37-41] Thus, one simple design approach to convert a ZF domain into a catalytic zinc site involves the modification of one of the four zinc coordinating ligands to allow for an open coordination site for substrate binding. This approach was previously attempted for CP-1, by Berg and co-workers,[42] who truncated the last four amino acids of CP-1. This truncation deleted one of the metal coordinating

histidine ligands, which was predicted to make the peptide hydrolytically active by providing an open site for water coordination. Although zinc(II) was shown to coordinate to this peptide, it was not catalytically active toward a chromogenic substrate, 4-nitrophenyl acetate (4-NA), suggesting that simple modification of a ZF was not enough to impart activity.[42] However, more recently, Suguira and co-workers took a different approach to convert a structural ZF peptide into a hydrolytically active peptide. Their approach involved mutating specific amino acids within a singular ZF domain of Sp1, rather than truncating the C-terminus. Several of these modified Sp1 domains exhibited hydrolytic activity toward carboxylic ester and circular DNA substrates when zinc was bound, providing compelling evidence that a structural ZF domain can be converted to a catalytic domain.[43-48] [38, 49, 50]

The intriguing catalytic activity reported by Sugiura and co-workers for the re-engineered Sp1 zinc-finger peptide motivated us to re-investigate CP-1 for possible conversion to a hydrolytically active peptide, since such a result would demonstrate that the most basic and general consensus sequence for a structural ZF protein domain is capable of sustaining catalytic activity. Instead of simply deleting a His ligand as done previously,[42] we sought to impart hydrolytic activity to CP-1 by modifying one of the zinc coordinating ligands. We chose to modify the second cysteine of CP-1 to an alanine (named CP-1(CAHH)), as this would result in a CP-1 variant that contains a ligand set that matches that of a known, hydrolytically active enzyme peptide deformylase (CHH).[41, 51] We demonstrate that this mutant, CP-1(CAHH), coordinates Zn(II) ion with high affinity, and also coordinates cobalt(II) ion. The binding of these divalent metal ions is found to induce partial folding of the peptide. It is shown that CP-1(CAHH)(M^{II}) (M = Zn, Co) exhibits good hydrolytic activity toward 4-NA, and mechanistic hypotheses for the observed hydrolytic reactivity are evaluated.

Results and discussion

Revisiting the consensus peptide.

The 'classical' ZF proteins, which are the best studied, contain domains with two cysteine and two histidine ligands. The overall form is (Tyr,Phe)-X-Cys-$X_{2,4}$-Cys-X_3-Phe-X_5-Leu-X_2-His-$X_{3,4}$-His, with X equaling any amino acid.[33] These proteins were first identified in the mid-1980s, before any comprehensive genome sequencing of whole organisms had been achieved.[52-54] In 1991, Berg and co-workers aligned all of the sequences of known ZFs, 131 sequences from 18 proteins, and identified a consensus peptide sequence (CP-1) with the sequence ProTyrLys**Cys**ProGlu**Cys**GlyLysSerPheSerGlnLysSerAspLeuValLys**His**GlnArgThr**His**ThrGly (Fig. 1 a-d). This sequence was shown to bind cobalt(II) and zinc(II) more tightly (lower K_d) than any native 'classical' ZF. Thus, CP-1 is considered the optimized 'classical' ZF.[33] CP-1 has subsequently been utilized for a variety of studies aimed at understanding topics ranging from the thermodynamics and kinetics of ZF protein folding, to the design of new ZF-based complexes.[31, 33-36, 55-57] A recent example is seen in the work of Sénèque and Latour, where CP-1 and a series of mutants were utilized to systematically measure binding affinities for Zn(II) and Co(II) ions by using competitive chelators, and to determine the kinetics of metal ion exchange and speciation.[36] Thus, the original CP-1, determined from a small subset of sequenced proteins, is a canonical ZF sequence and remains relevant to current work on ZF biochemistry.

An additional 13,465 CCHH ZF sequences have been identified since the initial report of CP-1, as a result of the proliferation of sequenced genomes from high-throughput proteomics efforts. The original CP-1 sequence was investigated here to determine if the peptide that was designed in 1991 from only 131 sequences is still the most conserved sequence. Using the

EXPasy program, all of the CCHH type ZF domains that have been sequenced and deposited in protein databases were extracted and aligned, and a Prosite Sequence Logo was then generated (Fig. 1A). A Sequence Logo is a visualization of the sequence conservation between homologous proteins. The output of a sequence logo shows a protein sequence with each amino acid represented at a specific height, which corresponds to units of 'bits' on the y-axis. The height of the amino acid indicates the frequency with which it occurs in that specific position throughout all of the sequences analyzed. When the amino acid is conserved at the 100% level, the height of the amino acid will be at its maximal level, which is 4 bits. When the amino acid is not conserved 100% of the time, several amino acids will be placed in a given column in the order of their percent conservation, with the most conserved amino acid appearing at the top.[58] Remarkably, a comparison of the new consensus sequence, CP-1(CCHH)-2015, with the original consensus sequence, CP-1(CCHH)-1991, shows a high degree of sequence conservation (Fig. 1B). Despite the small number of ZF sequences (less than 1% of those known today) analyzed by Berg and co-workers over twenty years ago, their original CP-1 sequence remains an accurate representation of a classical ZF domain. Thus the use of CP-1 was validated as a scaffold for the work described herein.

Modifying CP-1 to promote hydrolytic activity

Previous work from Berg attempted to make a mutation at the metal binding site of CP-1 to convert the structural zinc(II) site into a site capable of mediating hydrolysis.[42] CP-1 was truncated such that the last four amino acids were removed, including one of the histidine ligands, with the goal of opening up a site on the metal center for the binding and activation of H_2O. The activation of H_2O at Zn(II) in hydrolytic zinc enzymes, in which the pK_a of the bound

H_2O molecule is lowered, is a key part of their function and provides access to a nucleophilic Zn-OH species.[39, 40] No hydrolytic activity was observed in this earlier study, despite the successful formation of the CHH (NS_2) zinc center and the generation of an open coordination site at the zinc(II) ion in the CP-1(CHH) mutant.

Some of us have previously constructed hydrolytically active, synthetic (small-molecule) analogs of the active site of peptide deformylase (PDF).[59-61] This enzyme catalyzes the hydrolytic deformylation of the N-terminus of newly synthesized polypeptides. PDF is activated by the coordination of a divalent metal ion [Zn(II), Fe(II), or Co(II)] to one cysteine and two histidine residues (N_2S donor set) in the active site.[41, 51, 62] The activation of H_2O occurs at the metal center, ultimately leading to the hydrolysis of formylated substrates. We speculated that mutation of one of the Cys ligands in CP-1 to a non-coordinating residue would convert the metal site to an N_2S-M^{II} center and provide a mimic of the PDF active site that would have a higher Lewis acidity than the early CP-1(CHH) mutant. The Lewis acidities will directly influence the extent of water activation and the generation of the hydrolytically active zinc(II)-hydroxide species for CP-1() and CP-1(CAHH) according to equations 1 and 2, respectively.

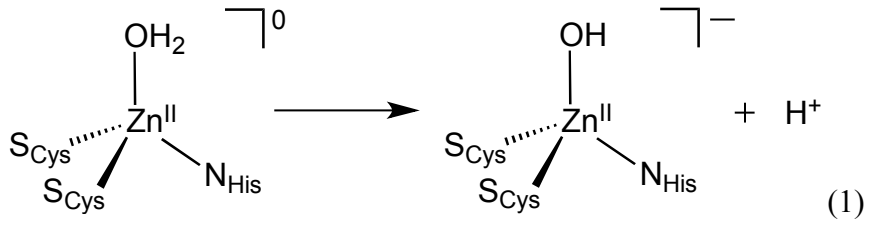

(1)

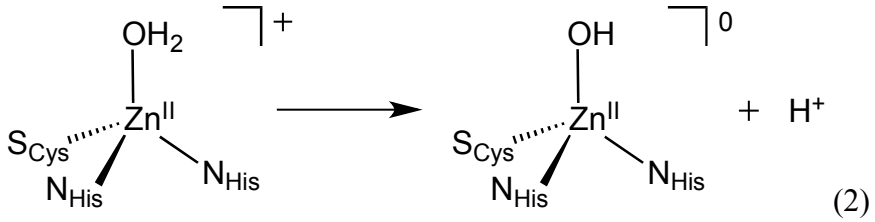

(2)

CP-1(CAHH) and coordination of Co(II)

CP-1 was modified to mimic the CHH metal binding motif of the active site of PDF. The native protein, referred to as CP-1(CCHH), was altered such that the second coordinating cysteine residue was mutated to a non-coordinating alanine residue [CP-1(CAHH)] (Fig. 1B). Initial attempts to synthesize this peptide independently by using a Symphony Quartet peptide synthesizer proved problematic. A significant portion of the peptide was not synthesized to completion, and separation of the incompletely synthesized peptide from the fully intact peptide via HPLC proved prohibitive due to low yields. The incomplete synthesis observed may be due to incomplete coupling of each amino acid or aggregation of the shorter peptides during synthesis. The peptide was then purchased from Bio-synthesis (Lewisville, TX) in the crude form and purified further in our laboratory by HPLC. This peptide was not soluble in the presence of metal ions. Pure, stable peptide was obtained from Biomatik (Wilmington, DE). The purity of the peptide was independently measured in our laboratory via analytical HPLC and found to be >95% pure. This peptide was utilized without further purification. We therefore note that the preparation of mutant CP-1 is not straightforward. Interestingly, Sénèque and Latour report similar difficulties in the preparation of CP-1 in their work.[36]

Initial experiments focused on determining the influence of the Cys-to-Ala mutation on the metal-binding properties of the peptide. The ability of CP-1(CAHH) to coordinate Zn(II) was determined indirectly by using Co(II) as a spectroscopic probe for Zn(II). This approach takes advantage of the rich spectroscopic properties of Co(II) in a tetrahedral coordination environment with sulfur and nitrogen ligands. The Co(II) (d^7) ion exhibits distinct *d-d* transitions between 550 – 750 nm that can be correlated with 4-coordinate, 5-coordinate, and 6-coordinate ligand environments around the metal. In addition, when sulfur, and to a lesser extent nitrogen,

serve as ligands, ligand-to-metal charge transfer (LMCT) bands are often observed in the near-UV region.[32, 63, 64]

Addition of $CoCl_2$ to CP-1(CAHH) at pH 7.5 leads to a spectrum that exhibits bands with maxima at 320, 530, and 630 nm (Fig. 2B). For comparison, we measured the UV-visible spectrum of Co(II) bound to a modified version of CP-1(CCHH) (Fig. 2A). This modified version, CP-1(CCHH)QΔW, which was created to investigate metal ion binding using fluorescence titrations in further experiments, contains a tryptophan residue in place of a glutamine as well as two additional amino acids at the C terminus (Fig 2A). The Co(II)-CP-1(CCHH)QΔW UV-visible spectrum is identical to that of Co(II)-CP-1(CCHH)-1991.[33] The *d-d* bands for Co(II)-CP-1(CCHH)QΔW and Co(II)-CP-1(CCHH)-1991 are red shifted with maxima at 570 nm and 645 nm compared to CP-1(CAHH) (Fig. 2B). The band at 320 nm remains the same. The position of the *d-d* transitions in relation to the coordination environment of the cobalt(II) ion has been well studied. It is known that cobalt(II) in a 4-coordinate, tetrahedral coordination geometry exhibits absorption maxima at 625 ± 50 nm, while cobalt(II) in a 6-coordinate, octahedral geometry gives maxima at 525 ± 50 nm. Cobalt(II) in a pentacoordinate geometry has maxima between these values.[63] While both the CCHH and CAHH CP-1 constructs exhibit absorbance maxima that best fit for tetrahedral coordination at cobalt(II), the absorbance bands for CP-1(CAHH) are blue shifted when compared to CP-1(CCHH), suggesting that the geometry may be distorted from an ideal tetrahedral environment to a 5-coordinate geometry. In addition, the extinction coefficient (ε) at the absorption maxima provides information about coordination number. Typically, tetrahedral complexes have an ε greater than 300 M^{-1} cm^{-1}, while octahedral complexes have an ε below 30 M^{-1} cm^{-1}, with the ε values for pentacoordinate complexes again falling somewhere in between 4- and 6-coordinate

complexes ($50 \leq \varepsilon \leq 250$ M^{-1} cm^{-1}).[43, 63] At its maxima, CP-1(CCHH) has an extinction coefficient of 510 M^{-1} cm^{-1}, suggestive of tetrahedral coordination. CP-1(CAHH) has a significantly lower extinction coefficient of 60 M^{-1} cm^{-1}, which is more consistent with a pentacoordinate (or even an octahedral) environment. Thus, in addition to the cysteine and two histidine residues, Co(II) [and, by inference, Zn(II)], is likely coordinated by one or two water molecules.

There is precedence for water coordination to zinc ions in re-engineered structural zinc sites. For example, when the second coordinating cysteine from a *de novo* four-helix bundle peptide called $Z\alpha_4$ that contained four pre-organized zinc binding ligands (Cys_2His_2) was mutated to an alanine, the Co(II) UV-visible spectrum was altered: the λ_{max} for the cobalt(II) *d-d* bands was blue-shifted to 592 nm from 617 nm observed for unmodified $Z\alpha_4$ and the extinction coefficient was decreased to $\varepsilon = 213$ M^{-1} cm^{-1} from $\varepsilon = 390$ M^{-1} cm^{-1}.[65] These data are suggestive of 5-coordinate geometry at the metal site, with two exogenous water molecules serving as ligands, in addition to the cysteine and histidine residues from the $Z\alpha_4$ ligand.[65] Modification of the first coordinating cysteine of $Z\alpha_4$ to an alanine also altered the absorption spectrum, with a measured extinction coefficient for the Co(II) *d-d* bands of $\varepsilon = 60$ $M^{-1}cm^{-1}$ (the λ_{max} was not reported). Similarly, Nomura and Sugiura found that when they systematically mutated metal coordinating cysteine and histidine ligands of the second ZF domain of Sp1 to non-coordinating ligands (alanine or glycine), the resultant metal site gave Co(II) UV-vis spectra consistent with a pentacoordinate geometry. The ligand sets of the Sp1 peptides were CCHG, CCAH, and CCGH respectively, and extinction coefficients (ε) of 191 $M^{-1}cm^{-1}$, 165 $M^{-1}cm^{-1}$, and 135 $M^{-1}cm^{-1}$ at 655, 620 and 625 nm for Co(II) coordination were reported.[43, 44] There are also examples of these types of metal centers in naturally occurring zinc enzymes. For example,

when Co(II) is bound to the zinc enzyme farnesyltransferase (FTase), the UV-vis spectrum exhibits a λ_{max} at 560 nm, with an extinction coefficient of 140 M^{-1} cm^{-1}, which is indicative of a 5-coordinate metal center with at least one water molecule bound to the metal.[66]

In addition to creating an open coordination site to which water can bind, it is not surprising that mutations that alter the metal binding site in ZFs have also been shown to affect the ZF's affinity for the metal ion. For instance, Klemba and Regan demonstrated that mutagenesis of the peptide $Z\alpha_4$ to favor pentacoordinate geometry at the metal site resulted in a 33-fold decrease in Co(II) ion binding affinity when compared to the Co(II) binding to the wild type $Z\alpha_4$ peptide.[65]

We thus performed spectroscopic titrations of CP-1(CAHH) with cobalt(II) ions to determine the effect of the alanine mutation on the affinity for metal ions (Fig. 3A). In this approach, the apo-peptide was titrated with cobalt(II) dichloride at pH 7.5 in 100 mM HEPES (50 mM NaCl) buffer until saturation was reached, as monitored by the appearance of the *d-d* transitions in the visible region. The resulting titration curve ($Abs_{630\ nm}$ versus [Co(II)], Fig. 3B) was easily fit to a 1:1 binding equilibrium, consistent with the formation of a 1:1 cobalt/peptide complex. The best fit of the data led to the determination of an upper limit for the dissociation constant (K_d) of 170 μM for cobalt(II) ion binding to CP-1(CAHH). In comparison, a K_d of 50 nM has been reported for CP-1(CCHH) when measured in the same manner while a $K_{apparent}$ of 10^{-15} M is reported when a more rigorous, competitive titration is performed.[36] Thus, the single Ala mutation in CP-1(CAHH) leads to a significant weakening of the binding affinity for Co(II) ions, but this result is not surprising given that one of the peptide-derived metal-binding ligands has been removed. Despite the deletion of one of the metal-binding Cys donors, the K_d for CP-

1(CAHH) is still within the regime of dissociation constants that have been reported for cobalt(II) coordination to ZF proteins.[36, 67, 68]

Zn(II) coordination of CP-1(CAHH)

The cobalt(II) ion was next used as a spectroscopic probe for measuring the binding of zinc(II) to CP-1(CAHH), which is spectroscopically silent. This strategy is well established for measuring zinc(II) binding affinities for ZF proteins.[19, 24, 28, 64, 68-71] A solution of fully loaded Co(II)-CP-1(CAHH) was prepared by combining the peptide with excess Co(II) ions (20 equiv of $CoCl_2$) at pH 7.5. Spectroscopic titrations were performed by the addition of successive aliquots of $ZnCl_2$, leading to the progressive loss of cobalt(II) *d-d* transitions at 630 and 550 nm. A plot of $A_{630\ nm}$ versus [$ZnCl_2$] is shown in Fig. 4A. The sharp decrease in the absorbance for the Co(II) marker band at 630 nm is indicative of displacement of Co(II) by Zn(II), confirming the coordination of Zn(II) by CP-1(CAHH). The lack of curvature in this plot indicates that the Zn(II) ion is binding very tightly in this concentration range, and the K_d for Zn(II) is too small to be measured with these data. These results for Zn(II) ion coordination to CP-1(CAHH) as compared to the Co(II) ion fall in line with other ZF proteins, in which the binding of Zn(II) is thermodynamically favored over that of Co(II) and typically has K_ds in the nanomolar to picomolar regime.[19, 28, 33, 34, 36, 56, 63, 67-69, 72-77]

Secondary structure of CP-1(CAHH) upon metal ion coordination

The binding of zinc(II) ions to ZFs can be expected to induce a structural change in the protein. ZF domains in the apo form are usually unstructured, only adopting secondary structure upon the coordination of a metal ion [e.g. Zn(II), Co(II)].[32, 78] The chemical shift dispersion of amide N-H

resonances can be correlated with the presence of secondary structural elements in small peptides and proteins,[79, 80] and the folding of CP-1(CAHH) was examined by 1-D (^{1}H) NMR spectroscopy in the presence and absence of zinc(II) ions. The 1-D (^{1}H) NMR spectrum for apo-CP-1(CAHH) is shown in Fig. 4B. The amide N-H peaks are found in the region 6.5 – 8.2 ppm and are not well dispersed, as expected for an unstructured peptide. The addition of one equivalent of $ZnCl_2$ to apo-CP-1(CAHH) at pH 7.5 resulted in shifts in the aromatic region, which are likely due to Zn(II) binding to the histidine ligands and some amide proton dispersion (Fig. 4C). It is well known that a slight lowering of the pH is often necessary to induce good dispersion in the amide N-H region associated with protein folding.[81] Additional dispersion of the amide N-H resonances was observed between 7.2 – 8.2 ppm upon lowering the pH to 6.0 and adding a slight excess of Zn(II) ions (4 equiv), as seen by comparison of the spectra for apo-CP-1(CAHH) and Zn-CP-1(CAHH) at pH 6.0 (Fig. 4D-E). Similar experiments have been performed with CP-1(CCHH) and the peaks corresponding to the amide N-H protons were dispersed over a wider range (6.5 – 9.4 ppm) upon metal ion coordination at pH 6.5.[36, 64] The NMR data indicate that CP-1(CAHH) clearly coordinates zinc(II) ions at pH 6.0 and exhibits some secondary structure formation upon metal ion binding, but does not fold to the same extent as CP-1(CCHH).

Hydrolysis of 4-nitrophenyl acetate (4-NA)

The ability of Zn(II)- CP-1(CAHH) and Co(II)- CP-1(CAHH) to mediate hydrolysis was examined with the test substrate 4-nitrophenyl acetate (4-NA). The 4-NA substrate has been commonly used to measure the hydrolytic efficiency of both zinc complexes, zinc peptides and proteins as well as other types of hydrolase mimics,[49, 59, 82-93] allowing for a direct comparison of the reactivity of CP-1(CAHH) against other hydrolytically active zinc complexes. The M-CP-

1(CAHH) [M = Zn(II) or Co(II)] peptide was incubated with 4-NA at pH 7.5 in 100 mM HEPES (1% acetonitrile, 50 mM NaCl) buffer and the hydrolysis reaction was monitored by UV-visible spectroscopy. All reactions were performed at 100 μM M-CP-1(CAHH). The desired reaction gives the expected product, 4-nitrophenolate (4-NP), which exhibits a characteristic absorbance at λ_{max} = 400 nm (ε = 12800 M^{-1} cm^{-1} at pH 7.5), appearing over time (Fig. 5). An initial rate method was employed to monitor the kinetics of hydrolysis of 4-NA. Initial rates (v_i) were obtained from the best-fit lines of [4-NP] versus time plots (Fig. 6). An initial rate method was selected because of the relatively slow rates observed for these reactions. The kinetics were measured over a range of substrate concentrations (0.5 – 2 equiv vs [M-CP-1(CAHH)]), and plots of $v_i/[\text{M-CP-1(CAHH)}]_0$ versus [4-NA] for both Zn(II)- and Co(II)-CP-1(CAHH) are shown in Fig. 7. The best-fit lines in Fig. 7 yield the second-order rate constants *k*" = 0.556 ± 0.072 M^{-1} s^{-1} and 0.482 ± 0.034 M^{-1} s^{-1} for the Co(II) and Zn(II) peptides, respectively (eq 5). These rate constants are on the high end of those reported for many zinc complexes, which mostly range from 0.036 – 0.6 $M^{-1}s^{-1}$ (Table 1).[59, 82, 84-87] The rates are comparable to those seen for the hydrolytic activity of mutant peptides based on the ZF domain of Sp1 reported by Nomura and Sugiura,[44] in which the metal-binding ligands were systematically varied (Table 1) and the hydrolytic cleavage of 4-NA was examined. Taken together, these data show that CP-1 can be re-engineered into a hydrolytically active peptide through ligand substitution at the metal center.

Conclusions

We have shown that the consensus peptide for a classical ZF domain, CP-1, can be modified by rational design to convert the structural zinc site into a zinc site capable of efficiently mediating the hydrolysis of an external substrate. The single mutation of Cys-to-Ala at the metal-binding site was made to give a CHH binding motif (CP-1(CAHH)), based on the known ligand set for the hydrolytically active Zn(II)/Fe(II) enzyme peptide deformylase. Despite the removal of one of the key metal binding ligands, CP-1(CAHH) is still capable of binding Co(II) and Zn(II) with good affinity, and shows some secondary structure formation upon binding metal ion, albeit less structurally ordered than the native CP-1(CCHH) peptide. The hydrolytic cleavage of the test substrate 4-NA mediated by M(II)-CP-1(CAHH) (M = Co, Zn) is faster than many of the known zinc model complexes that have been designed as catalytic mimics for zinc enzymes and tracks with the rates reported by Sugiura and co-workers for a modified Sp1 ZF peptide. We have thus shown that the CP-1 peptide represents a potential scaffold from which to create efficient, catalytically active hydrolysis enzymes that utilize biomimetic divalent metal ions. For high catalytic activity to be achieved, the non-coordinating amino acids may need to be optimized to promote hydrolysis at the zinc site as well as provide the proper structure to the catalytic domain. A systematic tuning of the metal active site and peptide structure by varying residues through a combinatorial and/or rational approach may lead to such optimization. We have shown that CP-1 may be an ideal system for this approach, given its high stability and its ability to tolerate mutations without loss of structural integrity.

Materials and methods

Identification of consensus sequence for CCHH ZFs (CP-1 update)

To determine an updated consensus classical ZF sequence, a search of "zinc finger" using PROSITE (prosite.expasy.org), which is part of the ExPASy suite of programs, was performed.[94, 95] From this search, a document 'PDOC00028,' which contains information about all CCHH-type ZF domains for which sequence information is available, was selected. The weblogo for the updated consensus sequence, named CP-1(CCHH)-2015 was generated via the 'retrieve the sequence logo from the alignment' link.[58, 96] This sequence logo was constructed from 13,465 true positive hits from the UniProtKB/Swiss-Prot databank and is shown in Fig. 1A.[97]

Peptide preparation

The CP-1(CAHH) peptide (PYKCPEAGKSFSQKSDLVKHQRTHTG) was purchased from Biomatik (Wilmington, DE) and stored in the solid form at -20 °C until use. A small amount of the solid peptide was resuspended in buffer prior to use and assayed for purity. A single peak was observed at 20% acetonitrile:80% water via High Performance Liquid Chromatography (HPLC). The identity of the isolated peak was confirmed by Matrix Assisted Laser Desorption Ionization-Time of Flight Mass Spectrometry (MALDI-TOF MS); [observed: 2931.23 (M^+); expected 2931.45]. The reduction state of the peptide was determined by measuring the ratio of total peptide to Co(II)-peptide. Typically, >95% of the peptide was reduced.[71, 98] The peptide was stored and manipulated under anaerobic conditions at all times (Coy Anaerobic Box, (95% N_2, 5 % H_2).

UV-visible metal binding titrations

Metal binding titrations were performed on a PerkinElmer Lambda 25 UV-visible spectrometer. In a typical experiment, $CoCl_2$ was titrated into a solution of apo-CP-1(CAHH) (600 μM in 1 mL) dissolved in HEPES (4-(2-hydroxyethyl)-1-piperazineethanesulfonic acid) (100 mM) with NaCl (50 mM) at pH 7.5. The titration included additions of 0.1, 0.2, 0.3, 0.4, 0.5, 0.6, 0.7, 0.8, 0.9, 1.0, 2.0, 5.0, 10, 15, and 20 molar equivalents of $CoCl_2$. The shape of the spectrum did not change during the course of the experiment, suggesting that Co(II) binds to the same site throughout the titration. A plot of A_{630} versus $CoCl_2$ was fit to a 1:1 binding model (equation 5) using non-linear least squares analysis (KaleidaGraph, Synergy Software). An upper limit dissociation constant (K_d) for cobalt(II) was determined.

(3) $$P + Co \rightleftarrows PCo$$

(4) $$K_d = \frac{[P][Co]}{[PCo]}$$

(5) $$[PCo] = \frac{[P]_{total} + [Co]_{total} + K_d - \sqrt{([P]_{total} + [Co]_{total} + K_d)^2 - 4[P]_{total}[Co]_{total}}}{2[Co]_{total}}$$

Where P = Peptide, Co = Cobalt. The ability of Zn(II) to displace Co(II) was determined by titrating Zn(II) into a solution of Co(II)-peptide (20:1 Co(II):peptide stoichiometry). As Zn(II) was titrated, the Co(II) *d-d* bands disappeared, indicating that Zn(II) was replacing Co(II) at the coordination site.

Nuclear magnetic resonance (NMR) spectroscopy

All NMR experiments were recorded on a 600 MHz Bruker spectrometer with the temperature maintained at 25 °C. Apo-CP-1(CAHH) and Zn(II)-CP-1(CAHH) (350 μM) were prepared in 25 mM deuterated Tris (tris(hydroxymethyl)aminomethane) containing 5% D_2O at pH 7.5 and at pH 6.0. The Zn(II)-(CAHH) samples included 1 and 4 equivalents of Zn(II) at pH values of 7.5 and 6.0, respectively. All of the NMR spectral data were processed using Spinworks software (http://www.umanitoba.ca./chemistry/nmr/spinworks).

Hydrolysis of 4-nitrophenyl acetate (4-NA)

The hydrolysis of 4-NA by the peptides was monitored using a PerkinElmer Lambda 25 UV-visible spectrometer by following the production of the reaction product, 4-nitrophenolate (4-NP), at 400 nm. Each reaction was performed in 100 mM HEPES, 50 mM NaCl, pH 7.5 with 1% acetonitrile. 100 μM M-CP-1(CAHH) [M = Zn(II) or Co(II)] (prepared at a 1:1 stoichiometry of M(II):peptide) was incubated with various concentrations of 4-NA (dissolved in acetonitrile) and the absorbance at 400 nm was recorded at 10 second intervals. The initial rate of hydrolysis was monitored up to a 5% yield of the product, 4-NP. Background hydrolysis was measured by incubation of 4-NA with either 100 μM $ZnCl_2$ or 100 μM $CoCl_2$ in the above buffer to determine if the metal ions alone could promote hydrolysis. In both instances, a low level of hydrolysis was recorded, and the appropriate spectrum for this hydrolysis was subtracted from the spectrum of the corresponding M-CP-1(CAHH) reaction with 4-NA. The method of initial rates was employed to monitor the reaction kinetics, and was then analyzed with the kinetic model shown in eqs 6 and 7:

$$v_i = k''[\mathrm{M-CP-1(CAHH)}]_0[4-\mathrm{NA}]_0 \qquad (6)$$

$$\frac{v_i}{[\mathrm{M-CP-1(CAHH)}]_0} = k''[4-\mathrm{NA}]_0 \qquad (7)$$

where ν_i = the initial rate of the reaction up to 5% conversion; $[\text{M-CP-1(CAHH)}]_0$ = initial concentration of metal peptide complex; $[\text{4-NA}]_0$ = initial concentration of substrate; *k*" = the second-order rate constant. The initial rate ν_i was obtained from linear fits of concentration vs time plots for 4-nitrophenolate (4-NP), where the concentration is given by $[\text{4-NP}] = A_{400}/\varepsilon \bullet l$ (ε = 12,800 M^{-1} cm^{-1}; l = 1-cm path length). Second-order rate constants (*k*" values) were determined according to eq 5 by taking the slopes of the best-fit lines of $\nu_i/[\text{M-CP-1(CAHH)}]_0$ vs [4-NA] [59, 60, 99]. All experiments were performed in triplicate.

Acknowledgments: SLJM would like to thank the NSF (CHE-1306208), ANB would like to thank the NIH (F31NS074768) and DPG would like to thank the NIH (GM062309, GM101153) for support of this research. We also acknowledge the Biomolecular NMR Center at JHU and Dr. Ananya Majumdar for assistance with NMR experiments

References

1. W. Shi and M. R. Chance, *Curr. Opin. Chem. Biol.*, 2011, **15**, 144-148.
2. S. M. Yannone, S. Hartung, A. L. Menon, M. W. Adams and J. A. Tainer, *Curr. Opin. Biotechnol.*, 2012, **23**, 89-95.
3. R. H. Holm, P. Kennepohl and E. I. Solomon, *Chem. Rev.*, 1996, **96**, 2239-2314.
4. A. C. Rosenzweig, *Chem. Biol.*, 2002, **9**, 673-677.
5. W. Maret, *J. Inorg. Biochem.*, 2012, **111**, 110-116.
6. W. Maret and Y. Li, *Chem. Rev.*, 2009, **109**, 4682-4707.
7. W. Maret, *Met. Ions Life Sci.*, 2013, **12**, 479-501.
8. W. Maret, *Adv. Nutr.*, 2013, **4**, 82-91.
9. C. Andreini, I. Bertini and G. Cavallaro, *PLoS One*, 2011, **6**, e26325.
10. I. Bertini, L. Decaria and A. Rosato, *J Biol Inorg Chem*, 2010, **15**, 1071-1078.
11. S. J. Lee and S. L. Michel, *Accts. Chem. Res.*, 2014, **47**, 2643-2650.
12. J. L. Michalek, A. N. Besold and S. L. Michel, *Dalton transactions*, 2011, **40**, 12619-12632.
13. J. H. Laity, B. M. Lee and P. E. Wright, *Curr. Opin. Struct. Biol.*, 2001, **11**, 39-46.
14. J. M. Matthews and M. Sunde, *IUBMB Life*, 2002, **54**, 351-355.
15. J. S. Hanas, D. J. Hazuda, D. F. Bogenhagen, F. Y. Wu and C. W. Wu, *J. Biol. Chem.*, 1983, **258**, 14120-14125.
16. J. Miller, A. D. McLachlan and A. Klug, *EMBO J.*, 1985, **4**, 1609-1614.
17. J. M. Berg, *Science*, 1986, **232**, 485-487.
18. J. M. Berg, *Proc. Natl. Acad. Sci. U. S. A.*, 1988, **85**, 99-102.
19. A. M. Rich, E. Bombarda, A. D. Schenk, P. E. Lee, E. H. Cox, A. M. Spuches, L. D. Hudson, B. Kieffer and D. E. Wilcox, *J. Am. Chem. Soc.*, 2012, **134**, 10405-10418.
20. K. L. Chan, I. Bakman, A. R. Marts, Y. Batir, T. L. Dowd, D. L. Tierney and B. R. Gibney, *Inorg. Chem.*, 2014, **53**, 6309-6320.
21. A. R. Reddi, T. R. Guzman, R. M. Breece, D. L. Tierney and B. R. Gibney, *J. Am. Chem. Soc.*, 2007, **129**, 12815-12827.
22. J. M. Berg, *J. Biol. Chem.*, 1990, **265**, 6513-6516.
23. J. M. Berg and Y. Shi, *Science*, 1996, **271**, 1081-1085.
24. J. M. Berg and H. A. Godwin, *Annu. Rev. Biophys. Biomol. Struct.*, 1997, **26**, 357-371.
25. D. Jantz, B. T. Amann, G. J. Gatto, Jr. and J. M. Berg, *Chem. Rev.*, 2004, **104**, 789-799.
26. A. N. Besold and S. L. Michel, *Biochemistry*, 2015, **54**, 4443-4452.
27. J. M. Berg and H. A. Godwin, *Annual review of biophysics and biomolecular structure*, 1997, **26**, 357-371.
28. J. C. Payne, B. W. Rous, A. L. Tenderholt and H. A. Godwin, *Biochemistry*, 2003, **42**, 14214-14224.
29. O. Seneque, E. Bonnet, F. L. Joumas and J. M. Latour, *Chemistry*, 2009, **15**, 4798-4810.
30. S. M. Quintal, Q. A. dePaula and N. P. Farrell, *Metallomics*, 2011, **3**, 121-139.
31. R. T. Doku, G. Park, K. E. Wheeler and K. E. Splan, *J. Biol. Inorg. Chem.*, 2013, **18**, 669-678.
32. A. D. Frankel, J. M. Berg and C. O. Pabo, *Proc. Natl. Acad. Sci. U. S. A.*, 1987, **84**, 4841-4845.

33. B. A. Krizek, B. T. Amann, V. J. Kilfoil, D. L. Merkle and J. M. Berg, *J. Am. Chem. Soc.*, 1991, **113**, 4518-4523.
34. B. A. Krizek, D. L. Merkle and J. M. Berg, *Inorg. Chem.*, 1993, **32**, 937-940.
35. B. A. Krizek, L. E. Zawadzke and J. M. Berg, *Protein Sci.*, 1993, **2**, 1313-1319.
36. O. Seneque and J. M. Latour, *J. Am. Chem. Soc.*, 2010, **132**, 17760-17774.
37. F. Yu, V. M. Cangelosi, M. L. Zastrow, M. Tegoni, J. S. Plegaria, A. G. Tebo, C. S. Mocny, L. Ruckthong, H. Qayyum and V. L. Pecoraro, *Chem. Rev.*, 2014, **114**, 3495-3578.
38. M. L. Zastrow and V. L. Pecoraro, *Biochemistry*, 2014, **53**, 957-978.
39. B. L. Vallee and D. S. Auld, *Proc. Natl.Acad. Sci. U. S. A.*, 1990, **87**, 220-224.
40. K. A. McCall, C. Huang and C. A. Fierke, *J. Nutr.*, 2000, **130**, 1437S-1446S.
41. K. T. Nguyen, J. C. Wu, J. A. Boylan, F. C. Gherardini and D. Pei, *Arch. Biochem. Biophys.*, 2007, **468**, 217-225.
42. D. L. Merkle, M. H. Schmidt and J. M. Berg, *J. Am. Chem. Soc.*, 1991, **113**, 5450-5451.
43. A. Nomura and Y. Sugiura, *Inorg. Chem.*, 2002, **41**, 3693-3698.
44. A. Nomura and Y. Sugiura, *Inorg. Chem.*, 2004, **43**, 1708-1713.
45. A. Nomura and Y. Sugiura, *J. Am. Chem. Soc.*, 2004, **126**, 15374-15375.
46. S. Negi, Y. Umeda, S. Masuyama, K. Kano and Y. Sugiura, *Bioorg. Med. Chem. Lett.*, 2009, **19**, 2789-2791.
47. S. Negi, M. Yoshioka, H. Mima, M. Mastumoto, M. Suzuki, M. Yokoyama, K. Kano and Y. Sugiura, *Bioorg. Med. Chem. Lett.*, 2015, **25**, 4074-4077.
48. M. Imanishi, S. Negi and Y. Sugiura, *Methods Mol. Biol.*, 2010, **649**, 337-349.
49. M. L. Zastrow, A. F. Peacock, J. A. Stuckey and V. L. Pecoraro, *Nat. Chem.*, 2012, **4**, 118-123.
50. M. L. Zastrow and V. L. Pecoraro, *J. Am. Chem. Soc.*, 2013, **135**, 5895-5903.
51. T. Meinnel, C. Lazennec and S. Blanquet, *J. Mol. Biol.*, 1995, **254**, 175-183.
52. F. Sanger, *Nat. Med.*, 2001, **7**, 267-268.
53. A. J. Simpson, *Nat. Rev. Genet.*, 2001, **2**, 979-983.
54. R. S. Brown, C. Sander and P. Argos, *FEBS Lett.*, 1985, **186**, 271-274.
55. C. A. Blasie and J. M. Berg, *Biochemistry*, 2004, **43**, 10600-10604.
56. C. A. Blasie and J. M. Berg, *Biochemistry*, 2002, **41**, 15068-15073.
57. C. A. Blasie and J. M. Berg, *Biochemistry*, 1997, **36**, 6218-6222.
58. T. D. Schneider and R. M. Stephens, *Nucleic Acids Res.*, 1990, **18**, 6097-6100.
59. R. C. diTargiani, S. Chang, M. H. Salter, Jr., R. D. Hancock and D. P. Goldberg, *Inorg. Chem.*, 2003, **42**, 5825-5836.
60. D. P. Goldberg, R. C. diTargiani, F. Namuswe, E. C. Minnihan, S. Chang, L. N. Zakharov and A. L. Rheingold, *Inorg. Chem.*, 2005, **44**, 7559-7569.
61. V. V. Karambelkar, C. Xiao, Y. Zhang, A. A. Sarjeant and D. P. Goldberg, *Inorg. Chem.*, 2006, **45**, 1409-1411.
62. P. T. Rajagopalan, S. Grimme and D. Pei, *Biochemistry*, 2000, **39**, 779-790.
63. I. Bertini and C. Luchinat, *Adv. Inorg. Biochem.*, 1984, **6**, 71-111.
64. J. M. Berg and D. L. Merkle, *J. Am. Chem. Soc.*, 1989, **111**, 3759-3761.
65. M. Klemba and L. Regan, *Biochemistry*, 1995, **34**, 10094-10100.
66. C. C. Huang, P. J. Casey and C. A. Fierke, *J. Biol. Chem.*, 1997, **272**, 20-23.
67. J. S. Magyar and H. A. Godwin, *Anal. Biochem.*, 2003, **320**, 39-54.
68. A. B. Ghering, J. E. Shokes, R. A. Scott, J. G. Omichinski and H. A. Godwin, *Biochemistry*, 2004, **43**, 8346-8355.
69. A. L. Guerrerio and J. M. Berg, *Biochemistry*, 2004, **43**, 5437-5444.
70. M. T. Worthington, B. T. Amann, D. Nathans and J. M. Berg, *Proc. Natl. Acad. Sci. U. S. A.*, 1996, **93**, 13754-13759.

71. S. J. Lee, J. L. Michalek, A. N. Besold, S. E. Rokita and S. L. Michel, *Inorg. Chem.*, 2011, **50**, 5442-5450.
72. S. L. Michel, A. L. Guerrerio and J. M. Berg, *Biochemistry*, 2003, **42**, 4626-4630.
73. A. N. Besold, A. A. Oluyadi and S. L. Michel, *Inorg. Chem.*, 2013, **52**, 4721-4728.
74. R. C. diTargiani, S. J. Lee, S. Wassink and S. L. Michel, *Biochemistry*, 2006, **45**, 13641-13649.
75. M. C. Posewitz and D. E. Wilcox, *Chem. Res. Toxicol.*, 1995, **8**, 1020-1028.
76. M. J. Lachenmann, J. E. Ladbury, J. Dong, K. Huang, P. Carey and M. A. Weiss, *Biochemistry*, 2004, **43**, 13910-13925.
77. A. N. Besold, D. L. Amick and S. L. Michel, *Mol. Biosyst.*, 2014, **10**, 1753-1756.
78. M. S. Lee, G. P. Gippert, K. V. Soman, D. A. Case and P. E. Wright, *Science*, 1989, **245**, 635-637.
79. K. Wuthrich, *Angew. Chem. Int. Ed. Engl.*, 2003, **42**, 3340-3363.
80. H. J. Dyson and P. E. Wright, *Annu. Rev. Phys. Chem.*, 1996, **47**, 369-395.
81. K. Wuthrich, 1986, **1**, 23-24.
82. C. Bazzicalupi, A. Bencini, A. Bianchi, F. Corana, V. Fusi, C. Giorgi, P. Paoli, P. Paoletti, B. Valtancoli and C. Zanchini, *Inorg. Chem.*, 1996, **35**, 5540-5548.
83. L. L. Kiefer and C. A. Fierke, *Biochemistry*, 1994, **33**, 15233-15240.
84. E. Kimura, I. Nakamura, T. Koike, M. Shionoya, Y. Kodama, T. Ikeda and M. Shiro, *J. Am. Chem. Soc.*, 1994, **116**, 4764-4771.
85. T. Koike, M. Takamura and E. Kimura, *J. Am. Chem. Soc.*, 1994, **116**, 8443-8449.
86. T. Koike, S. Kajitani, I. Nakamura, E. Kimura and M. Shiro, *J. Am. Chem. Soc.*, 1995, **117**, 1210-1219.
87. M. Subat, K. Woinaroschy, S. Anthofer, B. Malterer and B. Konig, *Inorg. Chem.*, 2007, **46**, 4336-4356.
88. K. L. Duncan and R. V. Ulijn, *Biocatalysis*, 2015, **1**, 67-81.
89. N. Singh, M. P. Conte, R. V. Ulijn, J. F. Miravet and B. Escuder, *Chem. Commun.*, 2015, **51**, 13213-13216.
90. B. Goyal, K. Patel, K. R. Srivastava and S. Durani, *RSC Advances*, 2015, **5**, 105400-105408.
91. C. M. Rufo, Y. S. Moroz, O. V. Moroz, J. Stohr, T. A. Smith, X. Hu, W. F. DeGrado and I. V. Korendovych, *Nature chemistry*, 2014, **6**, 303-309.
92. Y. Maeda, N. Javid, K. Duncan, L. Birchall, K. F. Gibson, D. Cannon, Y. Kanetsuki, C. Knapp, T. Tuttle, R. V. Ulijn and H. Matsui, *J Am Chem Soc*, 2014, **136**, 15893-15896.
93. C. Zhang, X. Xue, Q. Luo, Y. Li, K. Yang, X. Zhuang, Y. Jiang, J. Zhang, J. Liu, G. Zou and X. J. Liang, *ACS nano*, 2014, **8**, 11715-11723.
94. C. J. Sigrist, L. Cerutti, E. de Castro, P. S. Langendijk-Genevaux, V. Bulliard, A. Bairoch and N. Hulo, *Nucleic Acids Res.*, 2010, **38**, D161-166.
95. C. J. Sigrist, E. de Castro, L. Cerutti, B. A. Cuche, N. Hulo, A. Bridge, L. Bougueleret and I. Xenarios, *Nucleic Acids Res.*, 2013, **41**, D344-347.
96. G. E. Crooks, G. Hon, J. M. Chandonia and S. E. Brenner, *Genome Res.*, 2004, **14**, 1188-1190.
97. T. U. Consortium, *Nucleic Acids Res.*, 2012, **40**, D71-75.
98. S. J. Lee and S. L. Michel, *Inorg. Chem.*, 2010, **49**, 1211-1219.
99. S. A. Li, J. Xia, D. X. Yang, Y. Xu, D. F. Li, M. F. Wu and W. X. Tang, *Inorg. Chem.*, 2002, **41**, 1807-1815.

Table 1. Second order rate constants (k'') of the hydrolysis of 4-NA by various complexes and peptides.

Complex	k'' **(M^{-1} s^{-1})**	**Ref**
(PATH)ZnOH	0.089 ± 0003	58
([12]aneN_3)ZnOH	0.036 ± 0.003	83
(cyclen)ZnOH	0.1 ± 0.01	84
(CH_3cyclen)ZnOH	0.047 ± 0.001	85
([15]aneN_3O_2)ZnOH	0.6 ± 0.06	81
ZnL1	0.3908 ± 0.1	86
ZnL3	0.2791 ± 0.02	86
ZnL8	0.3863 ± 0.02	86
Protein/Peptide	k'' **(M^{-1} s^{-1})**	**Ref**
(His94Cys)CAII	117 ± 20	82
Zn(II)-Sp1(CCAH)	0.232 ± 0.0051	43
Zn(II)-Sp1(CCHA)	0.568 ± 0.0228	43
Zn(II)-Sp1(CGHH)	0.458 ± 0.0021	43
Zn(II)-Sp1(AHHH)	0.478 ± 0.0057	43
Zn(II)-Sp1(HHAH)	0.370 ± 0.0289	43
Zn(II)-Sp1(HHHH)	0.966 ± 0.0492	43
Zn(II)-CP-1(CAHH)	0.482 ± 0.034	This work
Co(II)-CP-1(CAHH)	0.556 ± 0.072	This work

Figure Captions

Fig. 1. Consensus peptide-1 (CP-1) constructs **A.** ExPASy output of all known CCHH zinc sites. **B.** The alignment of the amino acid sequences of CP-1 from 1991, CP-1 from 2015, and modified CP-1 [named CP-1(CAHH)] **C.** A cartoon figure showing the positions of the amino acids of CP-1(CCHH)-2015. The zinc coordinating residues are colored pink and the highly conserved amino acids are colored teal. **D.** The NMR structure of ZFP268, which is an example of a classical CCHH ZF protein. The zinc coordinating residues are colored pink and the highly conserved amino acids are colored teal. This figure was made in PyMol (v. 1.1), PDB ID: 2EMW.

Fig. 2. **A.** A sequence alignment of CP-1(CCHH) with CP-1-(CAHH). **B.** UV-visible spectra of Co(II)-CP-1(CCHH) QΔW. **C.** UV-visible spectra of Co(II)-CP-1(CAHH).

Fig. 3. **A.** Plot of the change in the absorption spectrum between 250-800 nm as 600 μM CP-1(CAHH) is titrated with $CoCl_2$. All spectrophotometric experiments were performed in 100 mM HEPES, 50 mM NaCl at pH 7.5 **B.** Plot of absorbance at 630 nm versus the concentration of $Co(II)Cl_2$ added to CP-1(CAHH). The data were fit to a 1:1 binding equilibrium to yield an upper limit dissociation constant of 170 μM. The solid line represents a nonlinear least-squares fit to the 1:1 binding model.

Fig. 4. **A.** Plot of absorbance at 630 nm versus the concentration of $ZnCl_2$ added to a saturated solution of Co(II)-CP-1(CAHH) [20:1 Co(II):CP-1(CAHH)]. All spectrophotometric experiments were performed in 100 mM HEPES, 50 mM NaCl at pH 7.5 **B.** ^{1}H-NMR spectrum of apo-CP-1(CAHH) at pH 7.5, **C.** ^{1}H-NMR spectrum of apo-CP-1(CAHH) with 1 equivalent of $ZnCl_2$ at pH 7.5, **D**. ^{1}H-NMR spectrum of apo-CP-1(CAHH) at pH 6, **E.** ^{1}H-NMR spectrum of apo-CP-1(CAHH) with 4 equivalents of $ZnCl_2$ at pH 6. The peptides for all NMR experiments were at a concentration of 350 μM in 600 μL of 25 mM deuterated Tris with 5% D_2O.

Fig. 5. A plot of the increase in the absorbance at 400 nM as 100 μM Zn(II)-CP-1(CAHH) reacts with 100 μM 4-NA to yield the chromogenic product 4-NP.

Fig. 6. A plot of 4-NP concentration ($A_{400}/(\varepsilon \bullet l)$) as a function of time indicating the production of 4-NP in the reaction of 100 μM 4-NA with Co(II)-CP-1(CAHH) (in blue), or Zn(II)-CP-1(CAHH) (in pink), all at 100 μM . All data were collected at pH 7.5 in 100 mM HEPES, 50 mM NaCl at 25 °C.

Fig. 7. Plot of ν_i/[M-CP-1(CAHH)] as a function of [4-NA] for the reaction of 4-NA with Co(II)-CP-1(CAHH) (blue line) and Zn(II)-CP-1(CAHH) (pink line). All data were collected at pH 7.5, 100 mM HEPES, 50 mM NaCl, 25 °C.

a

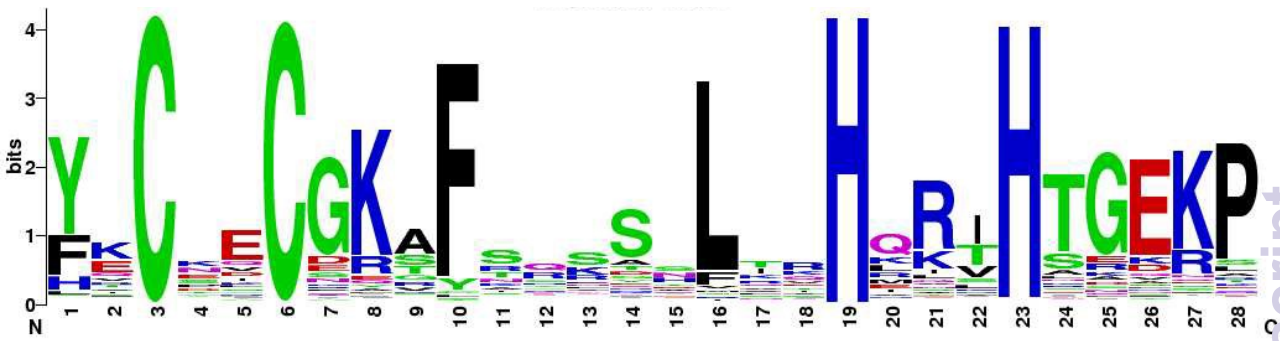

b

CP-1(CCHH)-1991	Y	K	C	P	E	**C**	G	K	S	F	S	Q	K	S	D	L	V	K	H	Q	R	T	H	T	G
MZF (CCHH)-1992	Y	A	C	A	A	**C**	A	A	A	F	A	A	K	A	A	L	A	A	H	A	A	A	H	A	K
CP-1(CCHH)-2015	Y	K	C	K	E	**C**	G	K	A	F	S	Q	S	S	S	L	T	R	H	Q	R	I	H	T	G
CP-1(CAHH)	Y	K	C	P	E	**A**	G	K	S	F	S	Q	K	S	D	L	V	K	H	Q	R	T	H	T	G

c

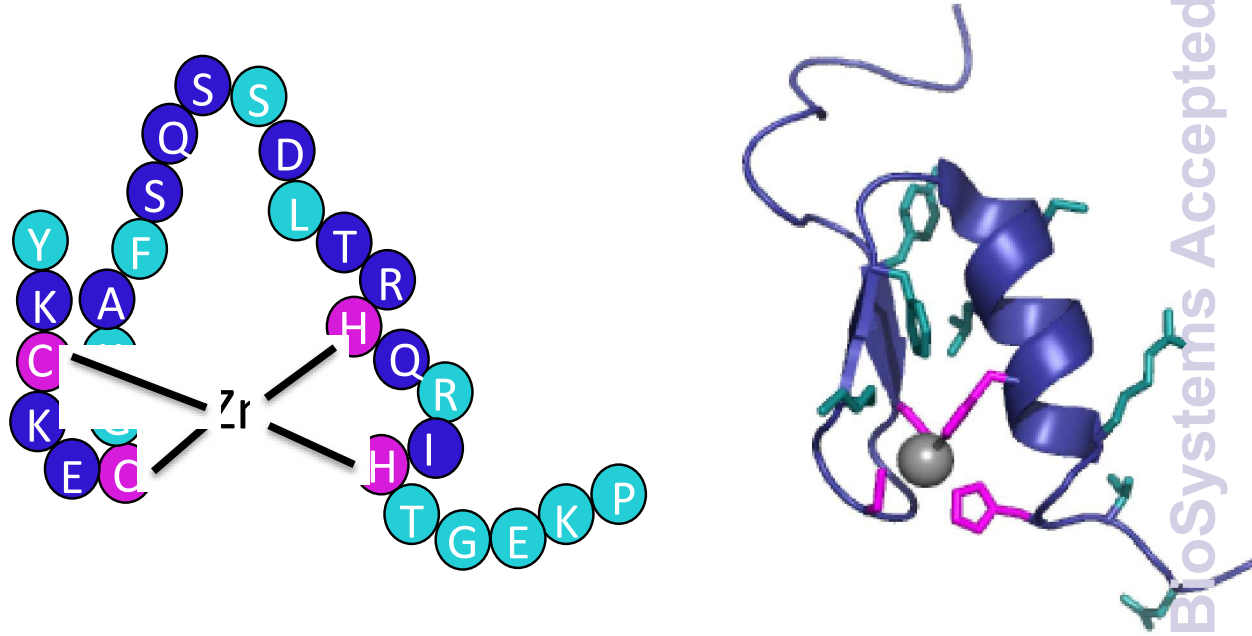

Figure 1.

a

```
CCHH  P Y K C P E C G K S F S Q K S D L V K H W R T H T G E K
CAHH  P Y K C P E A G K S F S Q K S D L V K H Q R T H T G
```

b

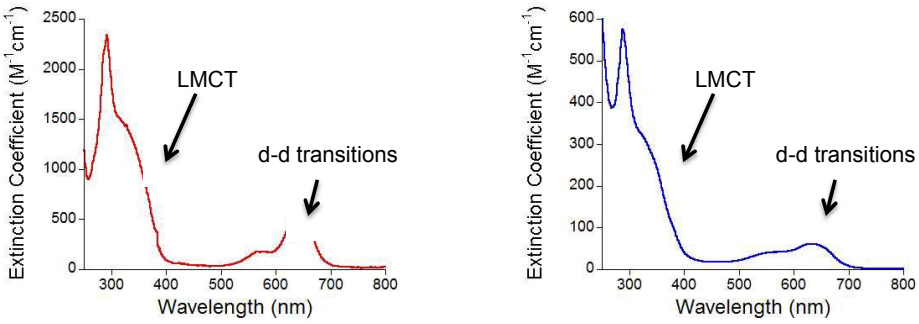

Figure 2.

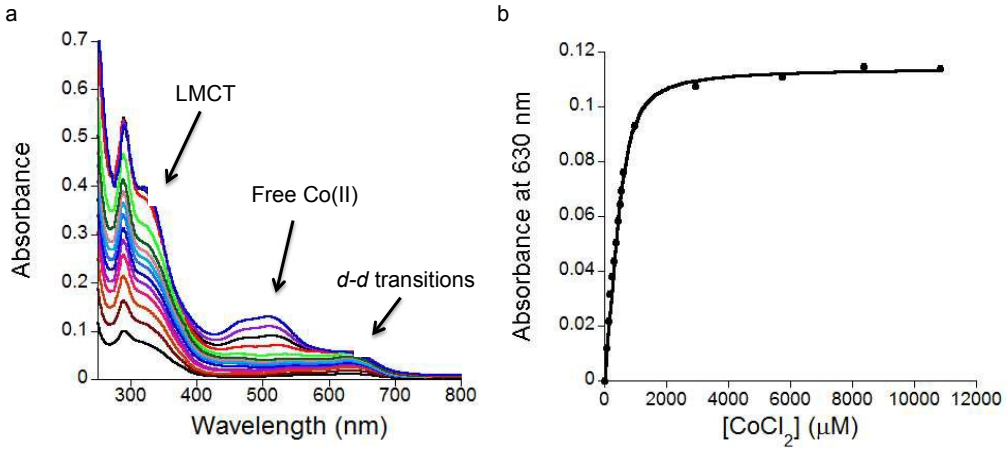

Figure 3.

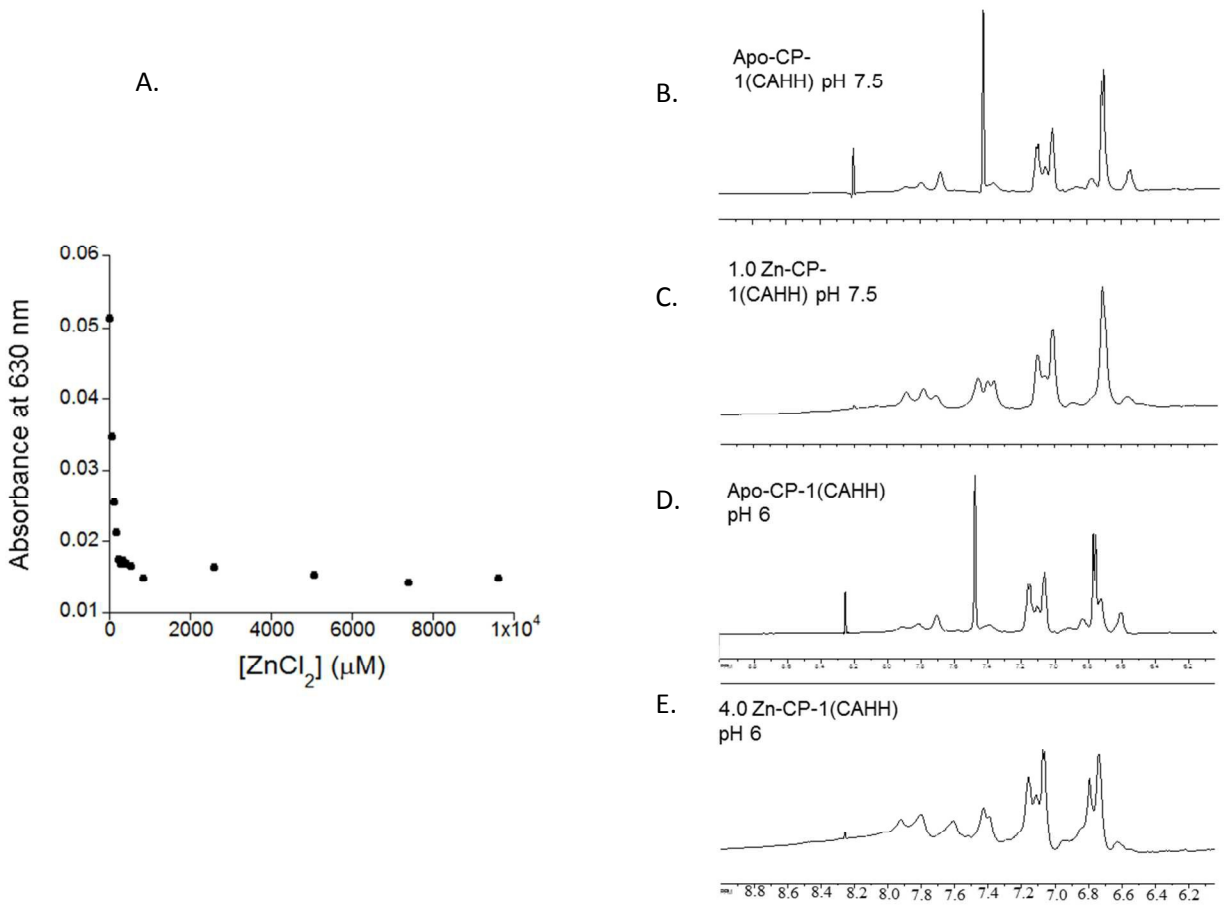

Figure 4.

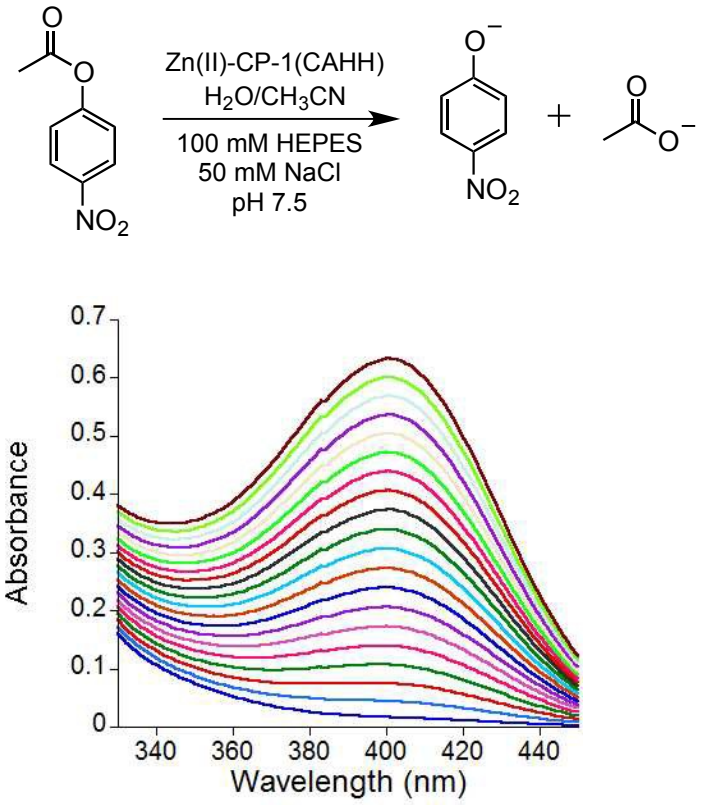

Figure 5.

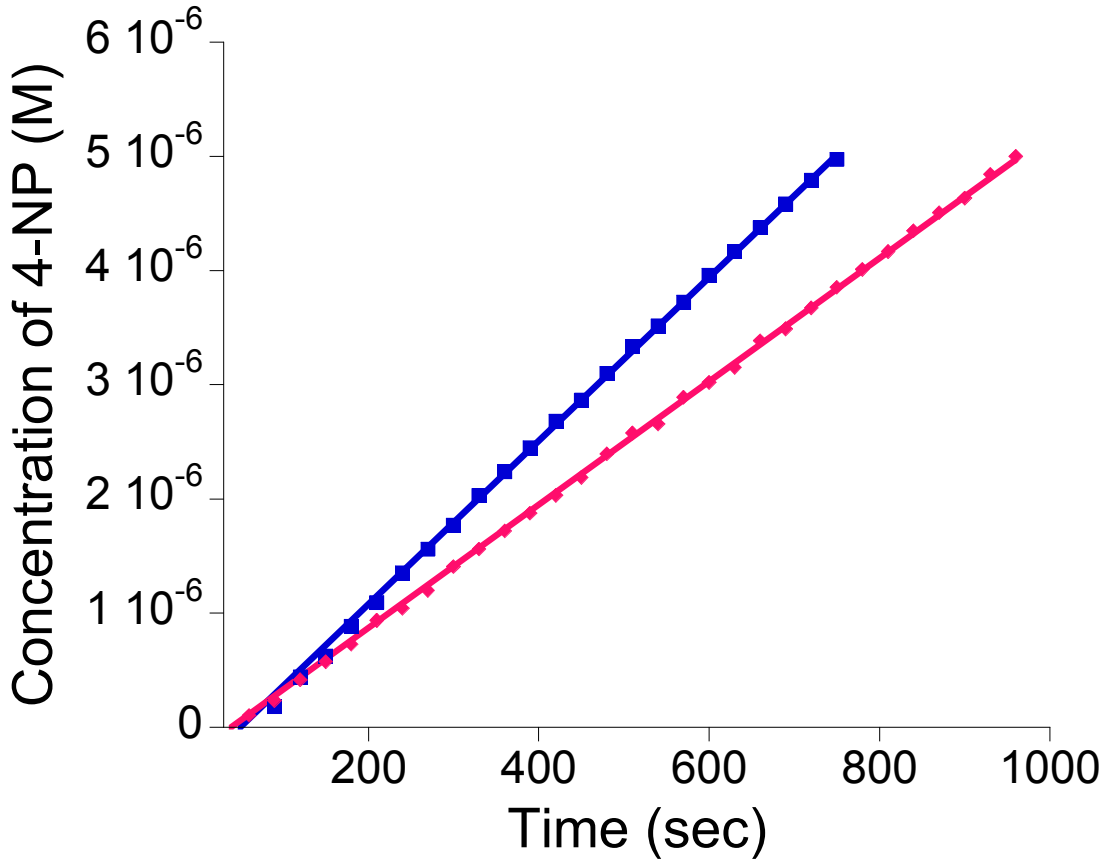

Figure 6.

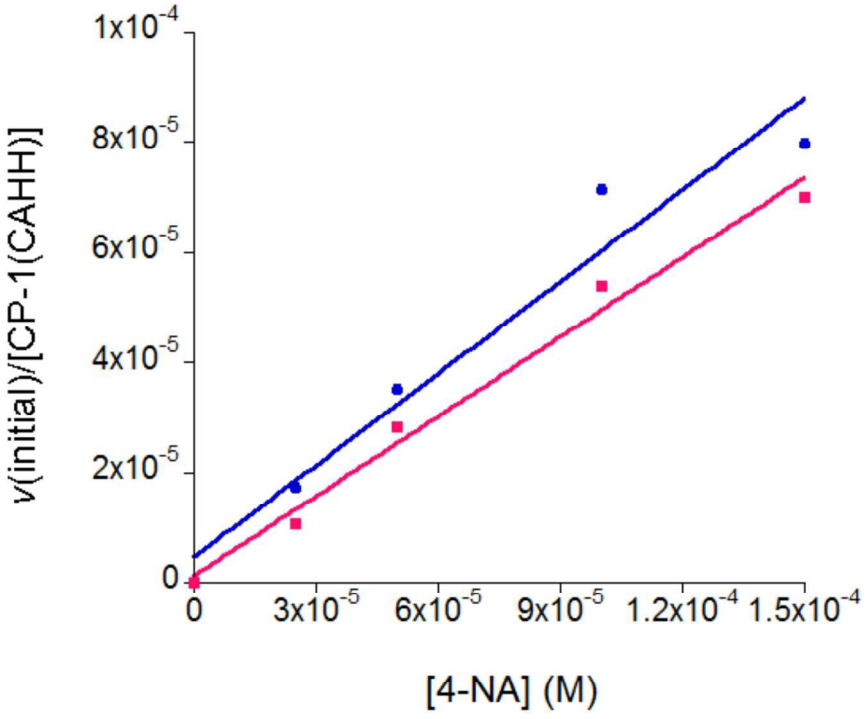

Figure 7.

TOC Graphic: